LA-UR -83-1083

5-5-83 WB

CONF-830606--5

Los Alamos National Laboratory is operated by the University of California for the United States Department of Energy under contract W-7405-ENG-36.

LA-UR--83-1083

DE83 011166

TITLE: PLASMA FOCUS EXPERIMENTS POWERED BY EXPLOSIVE GENERATORS

AUTHOR(S): B. L. Freeman, M-6
R. S. Caird, M-6
D. J. Erickson, M-6
C. M. Fowler, M-6
W. B. Garn, Consultant (M-6)
H. W. Kruse, P-14
J. C. King, M-6
D. E. Bartram, P-14
P. J. Kruse, P-14

SUBMITTED TO Will be submitted for presentation at Third International Conference on Megagauss Magnetic Field Generation and Related Topics, 13-17 June 1983, Novosibirsk, USSR.

Los Alamos

Los Alamos National Laboratory
Los Alamos, New Mexico 87545

FORM NO. 836 R4
ST. NO. 2629 5/81

MASTER

PLASMA FOCUS EXPERIMENTS POWERED BY EXPLOSIVE GENERATORS*

B. L. FREEMAN, R. S. CAIRD, D. J. ERICKSON, C. M. FOWLER, W. B. GARN, H. W. KRUSE, J. C. KING, D. E. BARTRAM, P. J. KRUSE

Los Alamos National Laboratory, Los Alamos, New Mexico 87545

ABSTRACT. Our plasma focus project began as an effort to develop an intense, pulsed, expendable neutron radiographic source. Since previous efforts to power a plasma focus with explosive generators had been successful, we proposed to couple our plate generators to a coaxial-geometry plasma focus to achieve this goal. Utilizing a small capacitor bank and a selected set of diagnostics, the explosive experiments were successfully conducted with maximum currents of 1.5 MA to 2.4 MA. A maximum neutron yield of ~ 3×10^{11} (DD) neutrons was achieved at the 2.4 MA level. Since the neutron yield did scale as a power of the maximum delivered current, and the neutron-producing source region was small, we conclude that this approach is an attractive option to achieve a neutron radiographic source. The need for a reliable open-circuiting switch at several megamperes has resulted in postponement of the project.

---

* Work supported by the U.S. Department of Energy

1. INTRODUCTION

The plasma focus project began as an effort to develop an intense, pulsed, expendable neutron radiographic source. The emphasis of the project was to devise such a source relatively quickly with limited resources. The plasma focus, with its impressive empirical scaling curve, was the logical device to use in achieving our goal. The desired neutron fluences implied that a coaxial dense plasma focus (Mather gun) must be operated with peak currents of 10 MA to achieve associated neutron yields of $> 10^{15}$ DD neutrons/pulse, Fig. 1. The expendable character of this source and the limits of our resources meant that explosive generator power supplies were attractive for both the development program and the final application. In the past, explosive spiral generators have been used by Beckner and Crawford [1] and Bernard et al. [2]. to supply the operating current for a plasma focus. The French group had achieved a neutron yield of $\sim 10^{9}$ DD neutrons/pulse with maximum currents of < 1 MA. In our context, a reasonable approach was to employ our fast plate generators for this application due to their much higher dL/dt characteristics and faster power pulse.

2. EXPERIMENTAL APPARATUS AND PROCEDURE

Given the speculative nature of this project, the effort has followed a progressive experimental program through increasingly higher current operational levels. This has provided for the physical understanding and development of high current plasma focus devices and steered the development of higher current explosive generator power supplies. In addition, extensive work with capacitor driven experiments preceeded all explosive generator shots.

The explosive flux compressors used in these tests were the plate-type generators (Fig. 2). Initial shots were performed with the small 26.4 cm long by 13.2 cm wide devices. The original nearly parallel plate configuration was altered for input/output separations of 7.12 cm and 12.7 cm, respectively. Later experiments employed the larger version of this flux compressor. This device is 52.8 cm long and 13.2 cm wide. The input/output plate separations were again 7.62 cm and 12.7 cm, respectively. This particular generator has an initial inductance of ~ 235 nH and is loaded with ~ 15 Kg of PBX-9501 explosive.

The indoor laboratory facility permitted capacitive drive of the plasma focus for parameter studies, diagnostic development, and conditioning for explosive tests. The capacitor bank stores 72 KJ of energy at 20 KV in 24, 14.7 μF modules. When configured with six gas switches and 72, 1.83 m, YK-198 cables, the inductance is ~ 9.8 nH. The maximum current delivered to a plasma focus is 1.0-1.1 MA, with a quarter period of ~ 4 μs. The entire pulsed power system was single-point grounded to provide a quiet environment for a reliable recording capability.

Our explosive pulsed power facility provides the necessary elements in a high-reliability context to fire relatively complex, single shot, explosive experiments. The initial flux source associated with this system consists of two 1470 μF capacitor banks. Each bank is simply cabled to fire through one detonator actuated switch. At 25 KV, each bank stores 459 KJ and has an inductance of ~ 60 nH. Like our indoor laboratory this facility is single-point grounded. It also provides limited support for mobile instrumentation trailers.

We selected the coaxial geometry plasma focus configuration (Fig. 3) and intentionally elected to operate the gun in the so-called high pressure mode. The coaxial gun has a center electrode (anode) diameter of 10.2 cm and an outer electrode internal diameter of 15.2 cm. The Pyrex insulator is 0.64 cm thick. Initially, this insulator was 5 cm long but was later lengthened to 7.6 cm, as a precautionary measure. The plasma focus anode length has been varied between 20.3 cm and 25.4 cm to accomodate the rundown times dictated by the power pulse characteristics and initial gas fill pressure. The outer electrode consists of 24, 38.1 cm long by 0.95 cm diameter bars with a reinforcing ring on the focus end. The inductance of the header and gun breech is ~ 2.6 nH.

The diagnostics employed in these experiments included the measurement of the full compliment of electrical characteristics, an extensive array of neutron detectors, and optical-image channel-plate intensifier cameras.

Currents were monitored on both the generator assembly and the plasma focus header with Rogowski coils. The gun voltage was measured using a shielded resistive probe with a frequency response of ~ 500 MHz. Neutron emission was characterized with activation methods, prompt and time-of-flight detectors, and a one-dimensional neutron imaging system. Silver, sulfur, and indium were used for activation measurements of total yield with a combined accuracy of ~ ±3%. Prompt and time-of-flight instruments were used to record the reaction history and energy spectra of the neutron yields. Lines-of-flight as long as 142 m both parallel and perpendicular to the plasma focus axis were used for energy resolution. The neutron imaging system was used to determine the neutron emission as a function of the position along the focus axis, beyond the end of the anode. Finally, and perhaps most important, the channel-plate cameras took $\leq$ 5 ns exposure, end-on optical images of the plasma sheath at two different times during the operation of the gun. These cameras provided much of the critical failure-mode information and many clues for correlating the other diagnostics into a unified picture of the experiments.

The procedure for firing a generator powered plasma focus shot typically required about five days to complete, but we were able to fire as often as once every three days. Initially, the necessary blast shielding was put into place, and grounding and diagnostics were laid out on the firing table. Once this was complete, parallel plate transmission lines were placed and connected to the focus header rings via 72, 4.27 m long RG-40/100 cables. Next, the explosive generator was set into place and connected to the transmission lines. Using the laboratory capacitor bank, the plasma focus device was preconditioned with a number of shots, usually

~ 50-75. When the explosive pulsed power supply was complete and the instrumentation was at full readiness, the plasma focus was prefilled to the initial pressure of deuterium for the test, sealed, and disconnected from the laboratory pulsed power and vacuum systems. The gun was then transported ~ 2.3 KM, attached to the header rings at the explosive facility, and fired within 30-90 min. At a more leisurely pace, the plasma device was returned to the indoor facility for cleaning and reconfiguration for the next test.

3. EXPERIMENTAL RESULTS

The total neutron yield for each shot was monitored with three activation techniques and an integrated reaction-history time-of-flight to an energy of 1 MeV. The shots that, in retrospect, were least influenced by adverse variables were III-2 ($Y_N = 4.5 \times 10^{10}$ neutrons; $I_{MAX} = 1.5$ MA), III-3 ($Y_N = 6.6 \times 10^{10}$ neutrons; $I_{MAX} = 1.9$ MA), and IV-2 ($Y_N = 2.0 \times 10^{11}$ neutrons; $I_{MAX} = 2.1$ MA). Other shots did produce neutron yields. In fact, the maximum yield obtained was 2.7×10^{11} neutrons with a maximum current of 2.4 MA, but we have reason to believe that this was a sub-optimal result due to a plasma sheath interaction with the vacuum chamber wall. The reason for the large array of detection methods was to ensure a cross-checked result for each event. An example of the agreements between these measurements is provided by shot III-3. For this test, the results for indium, sulfur, and silver activation were 6.7×10^{10} neutrons, 6.6×10^{10} neutrons, and 6.6×10^{10} neutrons, respectively. The integrated prompt neutron signal gave $\lesssim 9 \times 10^{10}$ neutrons. While this particular measurement yielded the largest variance on III-3, by the time IV-11 was fired the integrated prompt neutron result was identical to the activation measurement of 1.7×10^{11} neutrons.

The source distribution was observed along the axis of the plasma focus using a collimated, slitted fluor/photomultiplier technique. In Fig. 4A, one has an example of the data that is obtained from this instrument after the signals have been common-timed for shot IV-11. For this experiment, the detectors within this instrument; 50, 60, 70, 80, and 90; were viewing positions 1, 3, 6, 8.5, and 11 mm from the anode. We obtain Fig. 4B by taking snapshots in time and replotting the distribution data for IV-11 as position versus intensity. This result indicates that the centroid of the neutron producing region moves around appreciably, but that the time integrated neutron source is ~ 1-1.1 cm long for the bulk of the total yield.

Reaction history time-of-flight measurements were typically recorded at ~ 2.5 m and ~ 12 m from the focus region. The FWHM (full-width-half-maximum) of these signals varied from 48 ns on shot III-3 to 85 ns for shots IV-2 and IV-8. For IV-10 with the maximum neutron yield of 2.7×10^{11} neutrons, the FWHM was 64 ns. All of the shots producing significant neutron yield showed structure in the neutron pulse. Typically, a double peak was observed where the time separation was about 20-30 ns, Fig. 5.

Neutron energy spectra were obtained for both the radial and axial directions. With lines-of-sight $\gtrsim$ 140 m long, the time separation between the x-ray peak and the neutron pulse is ~ 6.2 μs. Typical data obtained from these detectors is given by Fig. 6A. For this test, detector 30 is the axial instrument and is bandwidth limited by an 8 MHz fiber optic link between the photomultiplier and the recording trailer. The radial detector, 40, was connected to the recording instrument with coaxial cable. Both detectors were located 141 m from the plasma focus. Transformation of these signals into the energy spectra (Fig. 6B) yields a peak in the axial spectrum at ~ 3.0 MeV and a peak in the radial spectrum at 2.3 MeV. The widths of these peaks were 0.53 MeV and 0.80 MeV for the axial and radial spectra, respectively. The radial result of 2.3 MeV is significantly lower than the expected value of 2.45 MeV. In addition to this aspect, there are several other, as yet, unresolved questions regarding the interpretation of this source of information.

Using the channel-plate camera in conjunction with other diagnostics, several key phenomena relating to the dynamics of the plasma sheath were observed. With the laboratory capacitor bank, we have been able to distinguish between the low and high pressure operational modes. In the low pressure mode, the plasma sheath is thick, diffuse, and ill defined. In addition to visible characteristics, the plasma focus performed erratically with large fluctuations in electrical and neutron-production characteristics from shot to shot. The high pressure mode resulted in a thin, sharply defined plasma sheath. Also, machine operation was quite consistent with highly reproducible operating parameters. In fact, after several years of operating a plasma focus with our 72 KJ bank, we have never observed a failure of this gun to perform normally in the high pressure mode that was not directly related to a capacitor bank malfunction.

In an early-time observation, we learned that at the time of plasma sheath formation the plasma expands radially from the end of the coaxial insulator more rapidly than elsewhere along its length. In fact, intensifier photographs indicate that this outward radial expansion may be as fast as > 20 cm/μs, as compared to axial sheath rundown velocities of 10-15 cm/μs. Two dimensional calculations with Lindemuth [3] have indicated that the cause of this behavior is simply the axial temperature profile of the current sheath as it begins its radial expansion during the inverse pinch. The plasma in this area is farther from potential contamination sources and is hotter.

The image intensifier cameras were essential to sorting out two contradictory behavior characteristics for the plasma focus operating under generator drive. The first of these resulted from the requirement of mobility for the experiment. Since the focus device was actually moved from the laboratory to the flux compression facility, efforts were made to reduce the weight and size of the gun. Thus, in the Series IV experiments, we used a 30 cm diameter vacuum chamber. At higher currents, > 2 MA, chamber asymmetries induced late-time breech discharges, Fig. 7. When the internal structure of the chamber was symmetrized, we achieved focus formation at slightly higher currents, but the same difficulty occurred again with a slight increase in current. With the Series V shots, we used a 65 cm diameter chamber, and this failure mode was not observed. Our interpretation is that a shock was reflected off the chamber wall, back into the electrode geometry, to cause a late-time breakdown in the focus breech.

The other sheath characteristic is tied to a relationship between $\dot{I}_o$ (the initial time-derivative of the current) and P_o (the initial gas pressure) that will permit stable propagation of the plasma sheath. If either the $\dot{I}_o$ is too low or the P_0 is too high, a second, asymmetrical plasma sheath will form behind the primary structure due to excessive residual gas remaining near the insulator. This will destroy the symmetry required for a focus to form. Stated differently, larger $\dot{I}_o$'s permit operation with higher P_o's, while reducing the residual gas behind the plasma sheath. This result is in good agreement with Fischer's [4] observation of coronal discharge characteristics at the time of plasma sheath formation.

An example of the voltage, current, and $\dot{I}$ signals (IV-2) are shown in Fig. 8. In all three traces, one observes the characteristic behavior associated with the focus pinch formation. However, there are some aspects of these quantities that reflect the nature of the plate-generator pulsed power supply. The initial $\dot{I}$ supplied to the gun is relatively low, ~ 0.5 MA/μs, but rather than trailing off, as with a capacitor drive, the $\dot{I}$ actually rises to ~ 0.8 MA/μs. As a result of this, the current rises in almost a straight line to a ~ 2.1 MA peak current. This is to be contrasted with the sinusoidal behavior of a capacitor bank. Of course, the voltage also rises with the higher $\dot{I}$, so the largest voltage appearing in the coaxial geometry is coincident with the highest currents, excepting the pinch behavior. The maximum power supplied to the plasma focus from the power supply in this case is ~ 59 GW.

4. DISCUSSION

The plasma focus project has now achieved a maximum neutron yield of $\sim 3 \times 10^{11}$ neutrons with a peak current of 2.4 MA. If the yields for shots III-2, III-3, and IV-2 are plotted on an empirical scaling curve against data obtained with capacitively driven systems, our results, even though single shot in nature, compare very favorably (Fig. 1). Our yields appear to scale as I^4 or I^5. These scaling results also compare quite well with those of Friewald and Downing [5], who demonstrated a scaling of V^5 on a capacitor facility.

Time-resolved neutron measurements produced two very encouraging results with the plasma focus operating in the high pressure mode. The neutron emitting region, as observed with the one-dimensional neutron imaging system, was short in axial length, ~ 1 cm long. Since this instrument was not turned to observe in the radial direction, we can not specify a source volume. Nevertheless, the measured length is in good agreement with the 5-12 mm long by 2 mm diameter source region reported by Trusillo et al. [6]. The FWHM of the neutron production history varied from 48 ns to 85 ns over the several experiments producing significant neutron yield. For the maximum yield of $\sim 3 \times 10^{11}$ neutrons, the FWHM was 64 ns. Both of these characteristics are desirable for a pulsed, neutron radiographic source. Ideally, one desires a point source of neutrons that is produced in a very short time. Currently, our spectral neutron information is puzzling, and further work will be required to understand its content. However, the axial detector clearly indicates that the source region is moving away from the anode. The one-dimensional source distribution measurement also indicates something of this nature.

A combination of plasma sheath observations and electrical diagnostics revealed that we are $\dot{I}_0$ or power limited at the time when the plasma focus is switched into the pulsed power circuit for the generator driven tests. Given a relationship between $\dot{I}_0$ and P_0, we have already observed that larger $\dot{I}_0$'s permit operation with higher P_0's while reducing the residual gas remaining in the breech region. Unfortunately, the limitations on the $\dot{I}_0$'s, that the generators used in these experiments can produce at 3-4 μs before burnout, imposed rather severe limits on the P_0's that would result in satisfactory plasma sheath performance. For example, the generator power supply used for the maximum currents of 2.4 MA provided only $\lesssim$ 1 MA/μs at switch time to the plasma focus. This is compatible with a P_0 of 5 torr, rather than the 10-15 torr desired for the peak current delivered. These usable gas pressures result in a transition toward the low pressure mode of operation late in the power pulse with the highest currents obtainable. This leads to a conclusion that we are $\dot{I}_0$-limited, early in the power pulse, in a manner which does not permit a compatible set of initial conditions. One way to overcome this difficulty is to use an open circuiting switch in the ballast inductor loop of the power supply circuit. A useful switch for plasma focus experiments would interrupt a few megamperes in $\lesssim$ 1 μs and remain open for the 3 to 4 μs pulse delivered to the device.

5. CONCLUSIONS

The plasma focus is a very promising device for a neutron radiographic source for three reasons. We have measured a neutron yield scaling proportional to I^{4-5}. The axial extent of the neutron producing region is small, < 1 cm. The FWHM of the neutron reaction history is short, < 100 ns.

We have observed the two dominant operating modes of a plasma focus, low and high pressure, and selected the high pressure mode as appropriate for the generator driven experiments. During the early phases of the inverse pinch, the plasma expands with a velocity > 20 cm/μs at the end of the insulator. The quantity of residual gas remaining behind the primary plasma sheath has been related to the interaction of the initial gas pressure and the initial time-derivative of the current.

This relationship forces us to conclude that the generator power supply imposed limits on the performance of the plasma focus. The power flow limitation at switch time imposed restrictions on the initial filling gas pressure and made it difficult-to-impossible to avoid a transition toward a low pressure operating mode for the higher current experiments. An open circuiting switch would provide an obvious remedy to this restriction, while making the generator power supply much more efficient in transferring current to its load. We have not observed any fundamental power flow limitations in the plasma focus.

ACKNOWLEDGEMENTS

We wish to thank Jerry Miller, Ron Buchanan, Robert Martin and Dennis Vasilich of Los Alamos for providing invaluable assistance with the neutron activation measurements. Joseph Mather provided vital information in the early stages of our effort to get our first plasma focus devices built and operating. Winston Bostick helped our understanding of the power flow in the plasma focus device through extensive discussions.

REFERENCES

[1] FOWLER, C. M., CAIRD, R. S. , ERICKSON, D. J., FREEMAN, B. L., THOMSON, D. B., GARN, W. B., in Second International Conference on Energy Storage, Compression, and Switching, Vo. 2, Plenum Press, New York (1983) 19.

[2] BERNARD, J., BOUSSINESQ, S., MORIN, J., NAZET, C., PATOU, C., VEDEL, J., Phys. Rev. Lett. 35A, 4 (1971) 288.

[3] LINDEMUTH, I. R., FREEMAN, B. L., in 1981 IEEE International Conference on Plasma Science (Santa Fe, NM, May 18-20, 1981) 61.

[4] FISCHER, H., HAERING, K., Applied Optics 18, 13 (July 1, 1979) 2258.

[5] FRIEWALD, D. A., DOWNING, J. N., A Survey of a 210-KJ Dense Plasma Focus (DPF-6), LA-5635 MS (June, 1974).

[6] TRUSILLO, S. V., GUZHOVSKII, B. YA., MAKEEV, N. G., TSUKERMAN, V. A., JETP Lett. 33, 3 (February 5, 1981) 140.

[7] ZUCKER, O., BOSTICK, W., GULLICKSON, R., LONG, J., LUCE, J., SAHLIN, H., The Design of a Repetitively Pulsed Megajoule Dense-Plasma Focus, UCRL-51872 (August 1, 1975).

FIGURE CAPTIONS

Figure 1. Neutron yield versus peak current per pulse [7]. Shots III-2, III-3, and IV-2 are plotted as solid circles.

Figure 2. Schematic of a trapezoidal plate generator power supply to drive a plasma focus. The input of the generator is crowbarred with first plate motion. The detonator switch connects the plasma focus in parallel with the ballast load at 3-4 μs before generator burnout.

Figure 3. Schematic of the plasma focus used in these experiments.

Figure 4A. Composite plot from the various detectors (axial positions) in the one-dimensional neutron imaging diagnostic for the neutron production intensity versus time.

Figure 4B. Six snapshots in time of the neutron production intensity versus distance from the anode.

Figure 5. Neutron time history at 2.5 m from the plasma focus for shot IV-11.

Figure 6. Data from the 141 m time-of-flight axial and radial neutron detectors for shot IV-8. 6A is the common timed detector current versus time. 6B shows the neutron energy spectra for this shot.

Figure 7. End-on gated channel-plate camera photographs of the plasma sheath during rundown and initial collapse. 6A is 1.49 μs after the plasma focus has been switched into circuit. 6B is 2.79 μs in time and shows a late-time breech breakdown due to a vacuum chamber asymmetry.

Figure 8. Characteristic (8A) voltage, (8B) current time-derivative, and (8C) current traces versus time for shot IV-2.

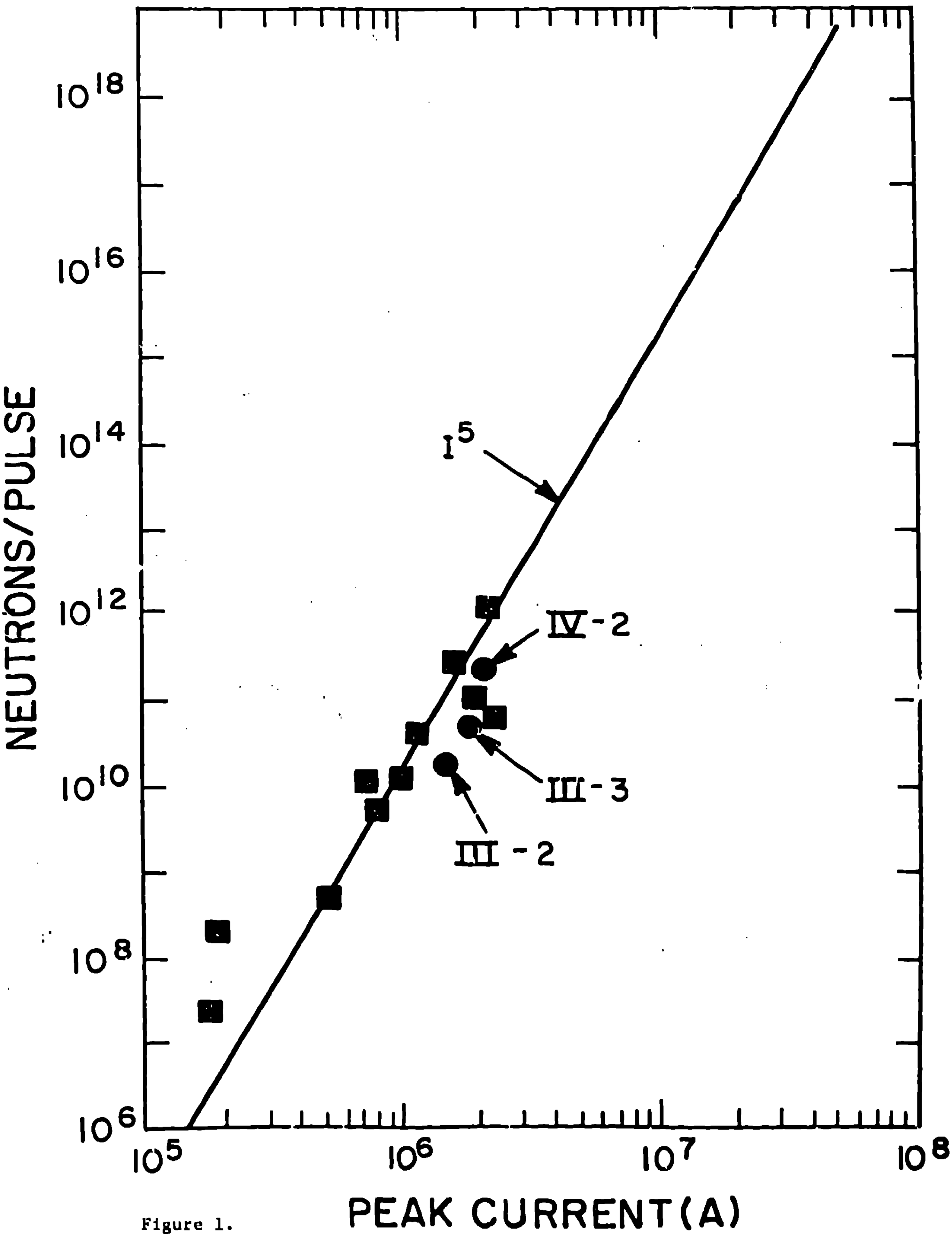

NEUTRONS/PULSE
10^18
10^16
10^14
10^12
10^10
10^8
10^6
10^5
10^6
10^7
10^8
PEAK CURRENT(A)
I^5
IV-2
III-3
III-2

Figure 1.

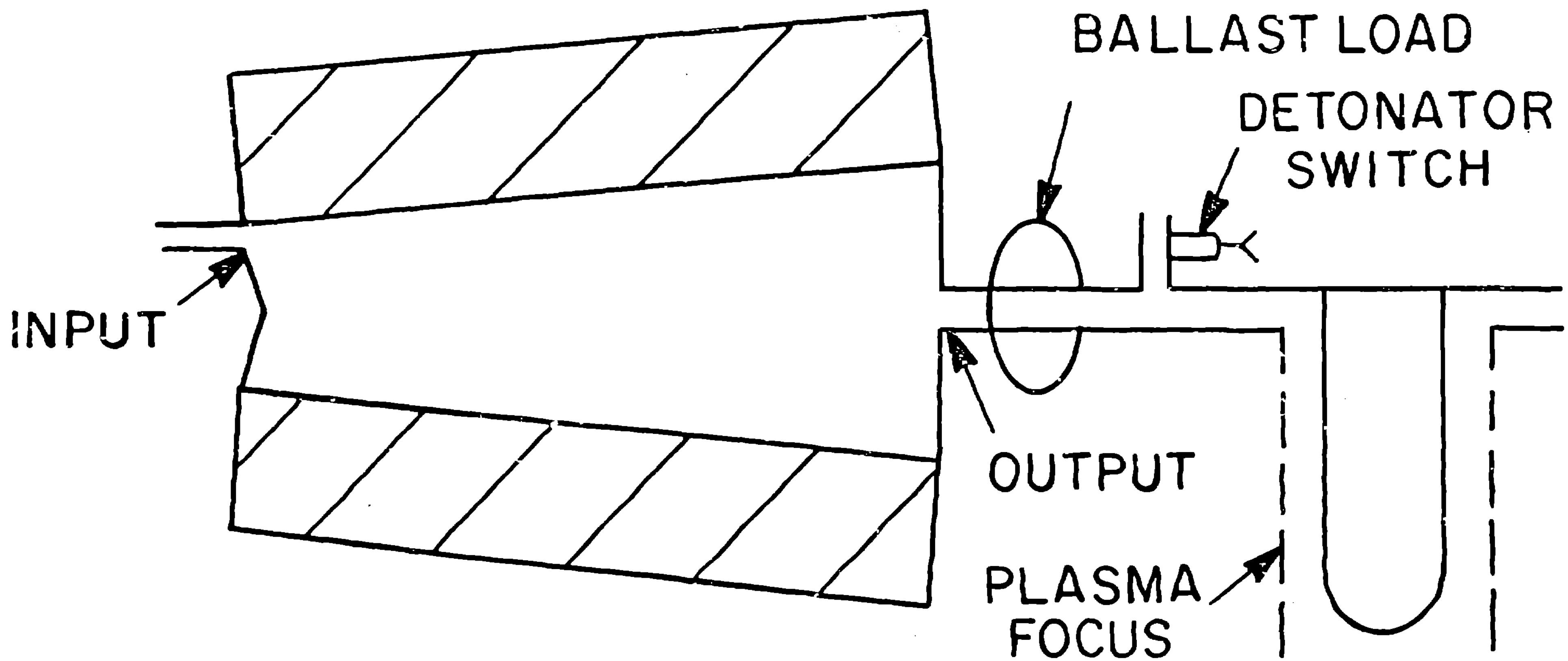

Figure 2.

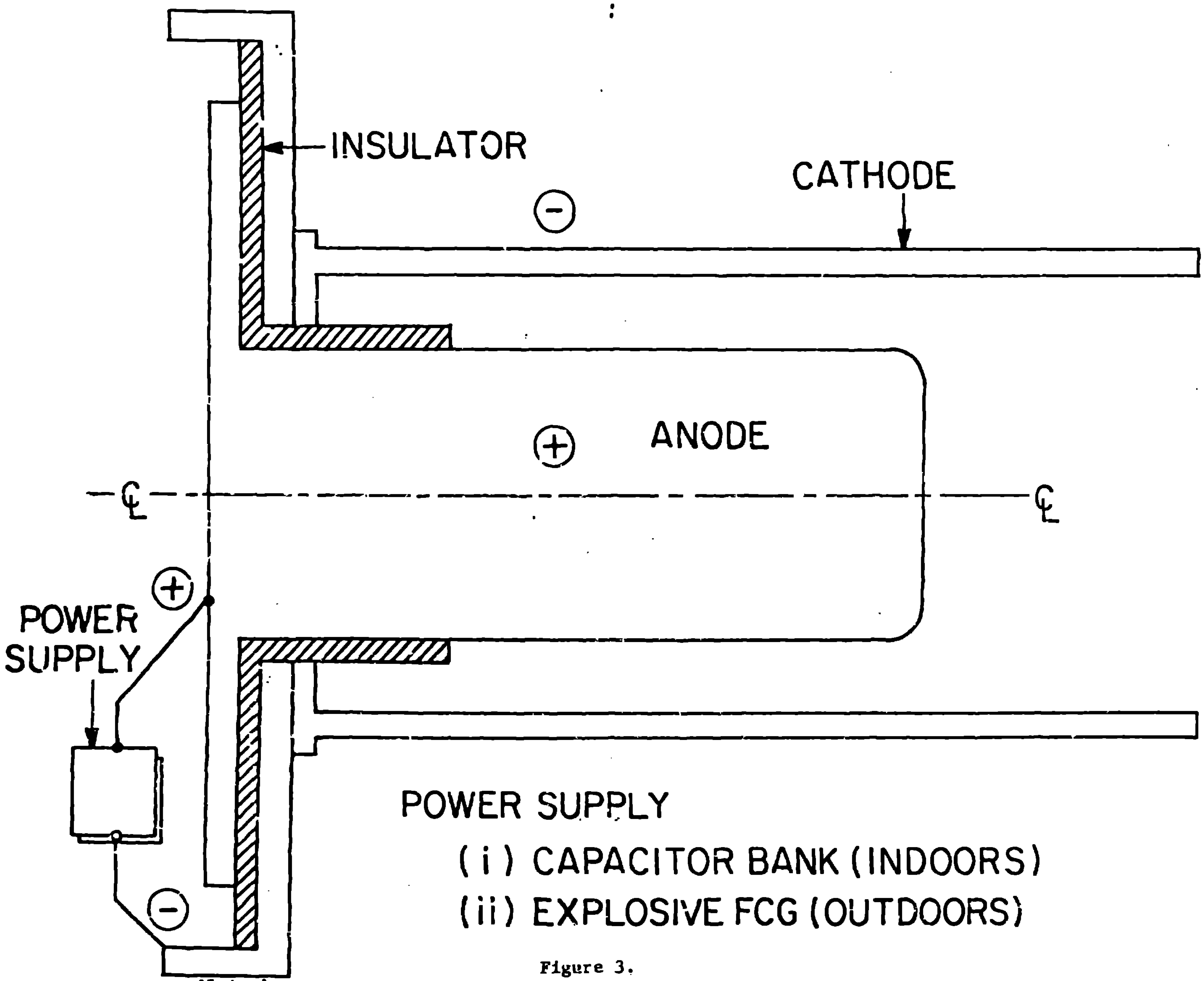
INSULATOR
CATHODE
ANODE
POWER SUPPLY
POWER SUPPLY
(i) CAPACITOR BANK (INDOORS)
(ii) EXPLOSIVE FCG (OUTDOORS)

Figure 3.

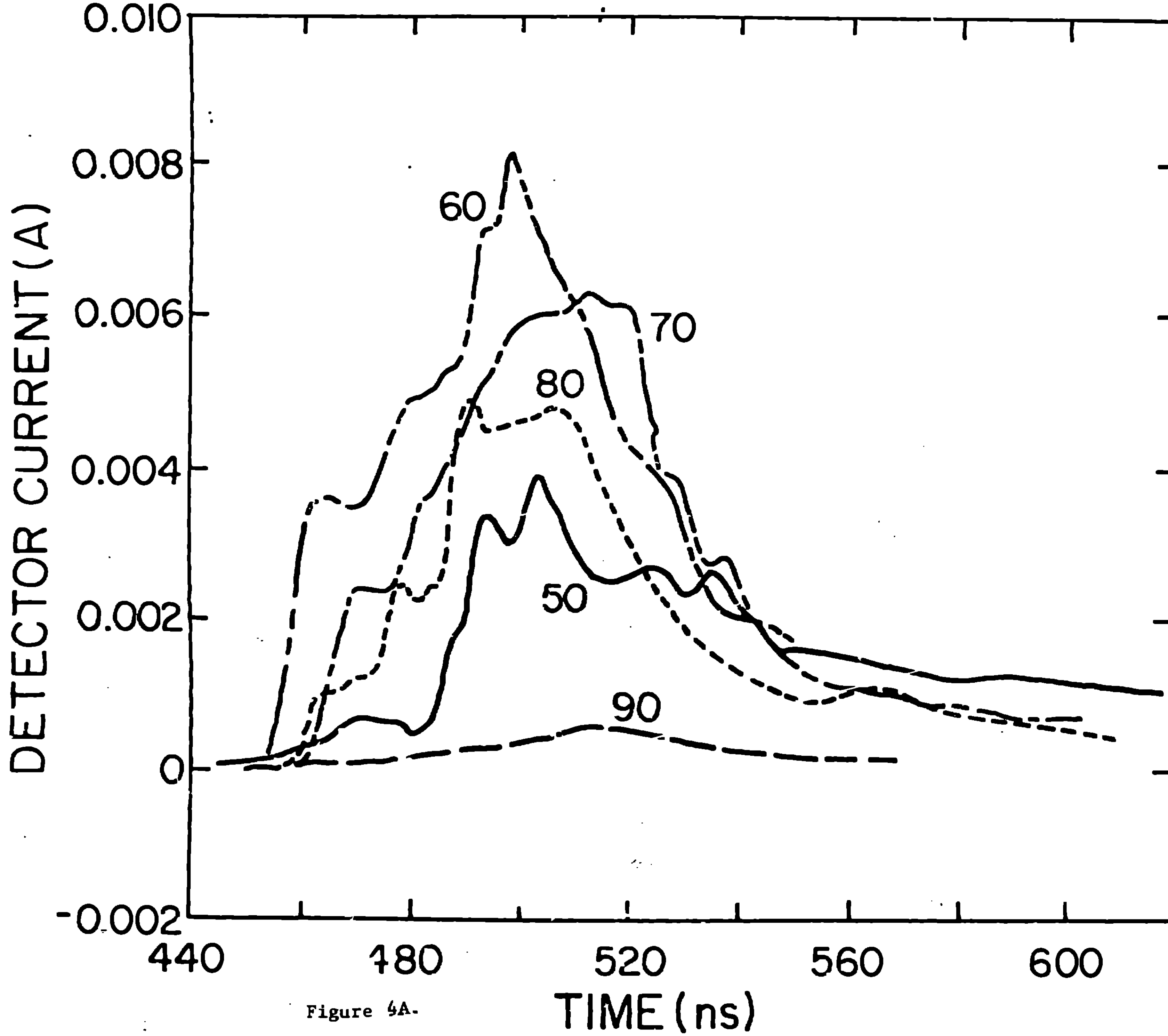

0.010
0.008
0.006
0.004
0.002
0
-0.002
DETECTOR CURRENT (A)
60
70
80
50
90
440
480
520
560
600
TIME (ns)

Figure 4A.

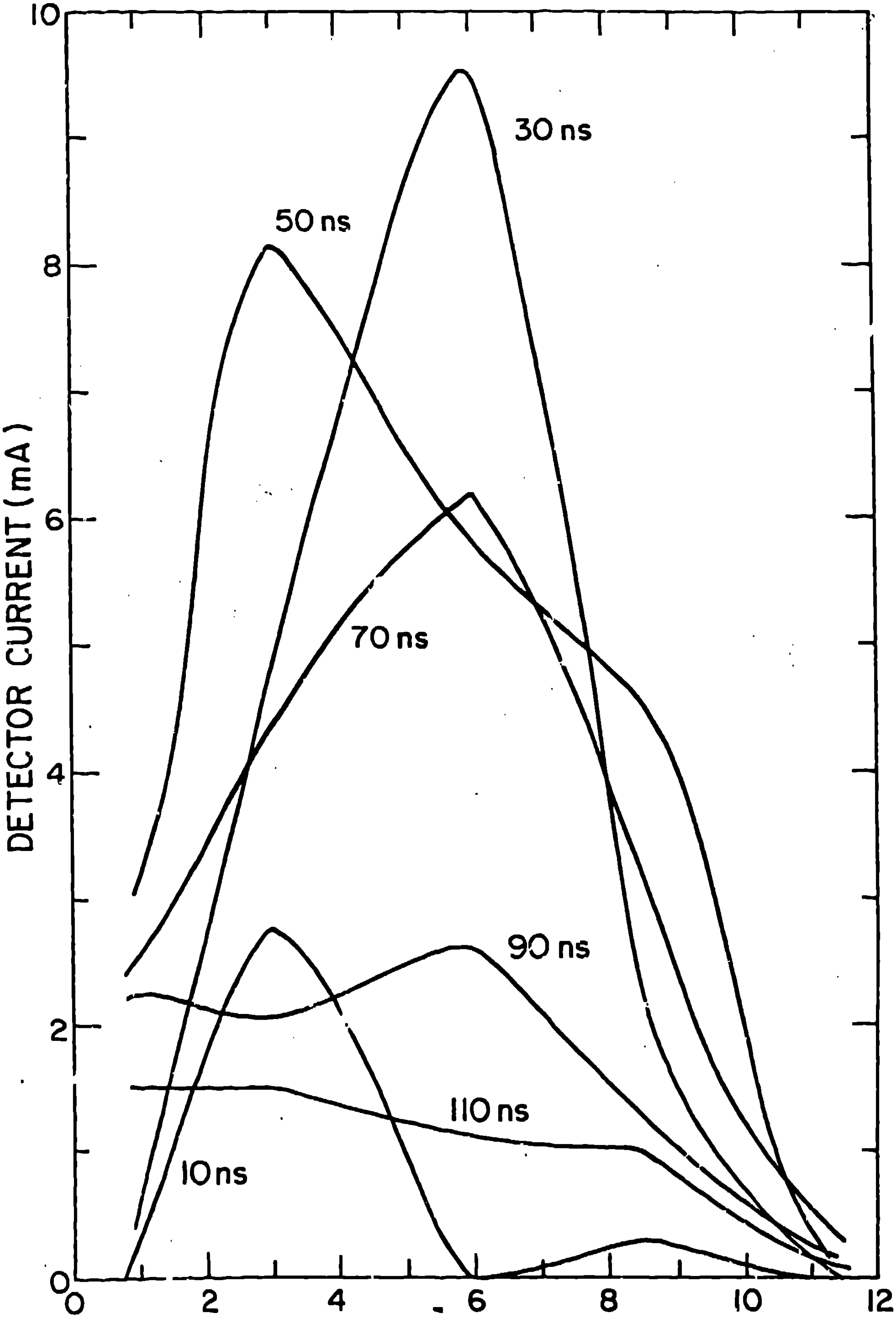

DETECTOR CURRENT (mA)
DISTANCE FROM ANODE (mm)
30 ns
50 ns
70 ns
90 ns
110 ns
10 ns

Figure 4B.

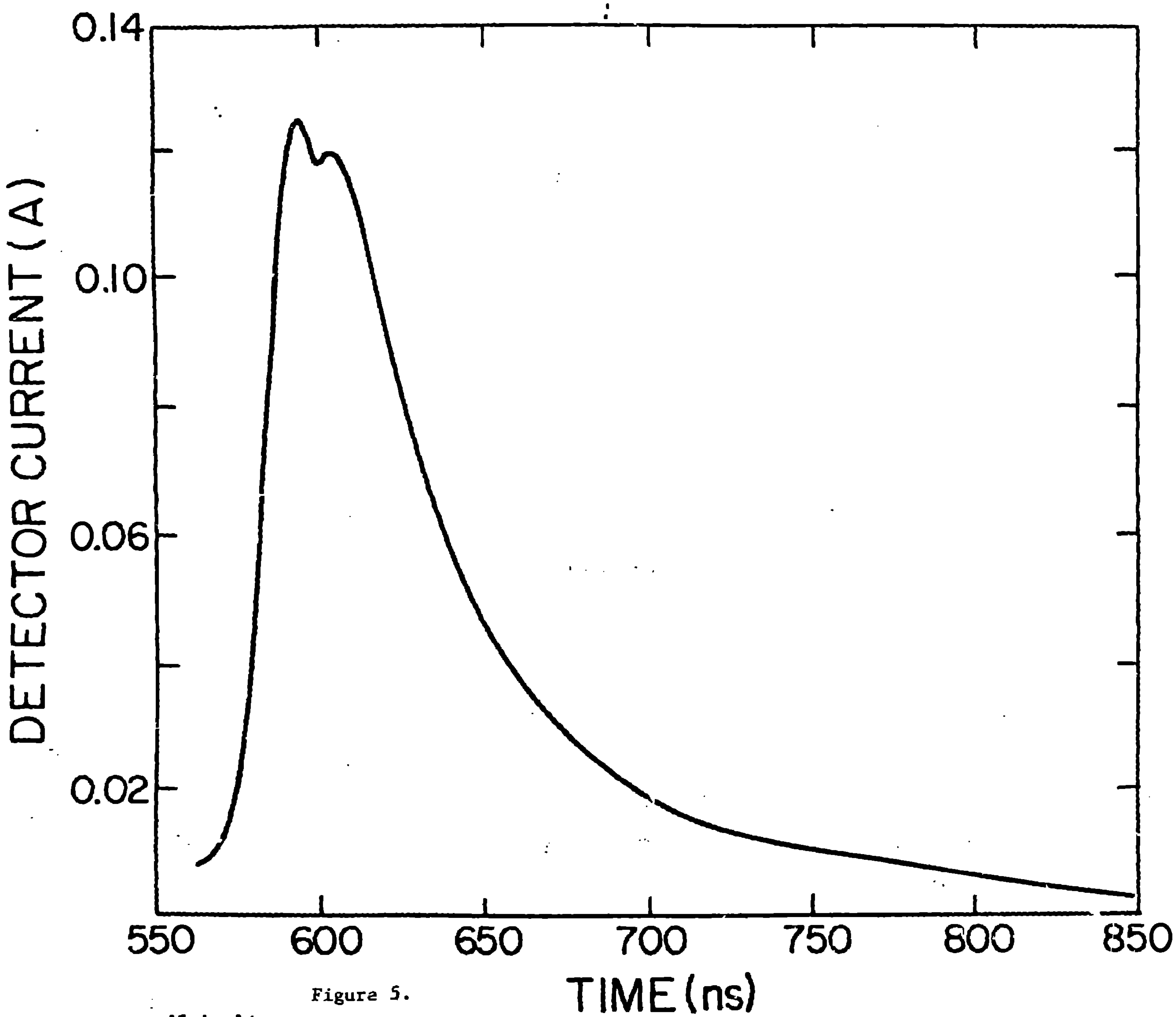

0.14
0.10
0.06
0.02
DETECTOR CURRENT (A)
550
600
650
700
750
800
850
TIME (ns)

Figure 5.

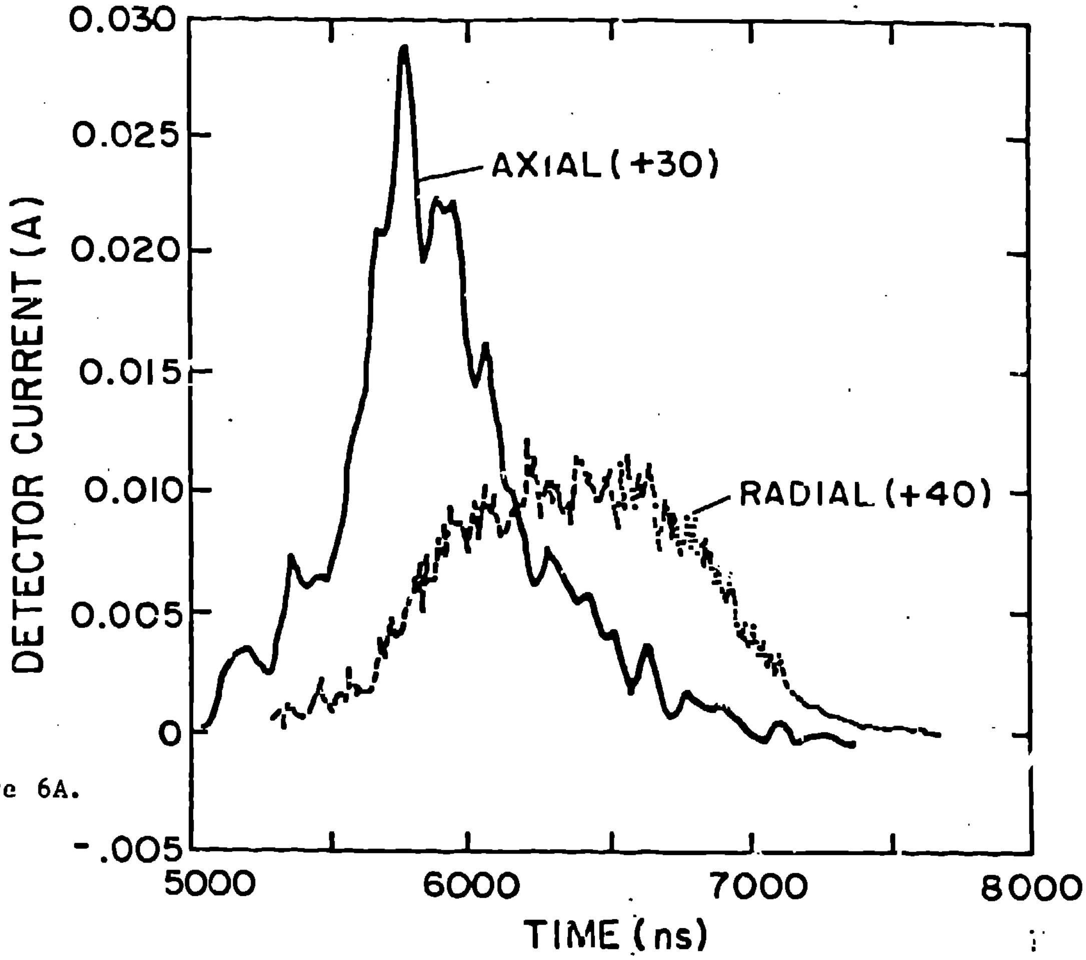

Figure 6A.

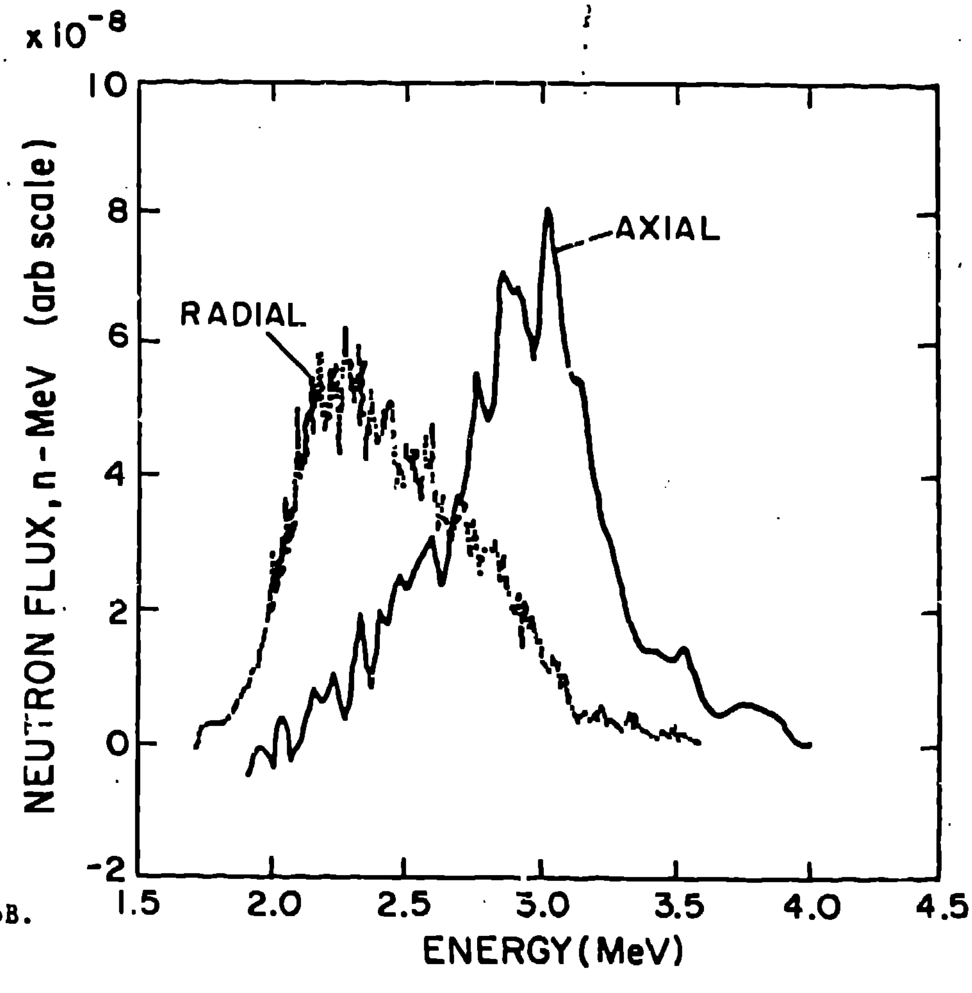

Figure 6B.

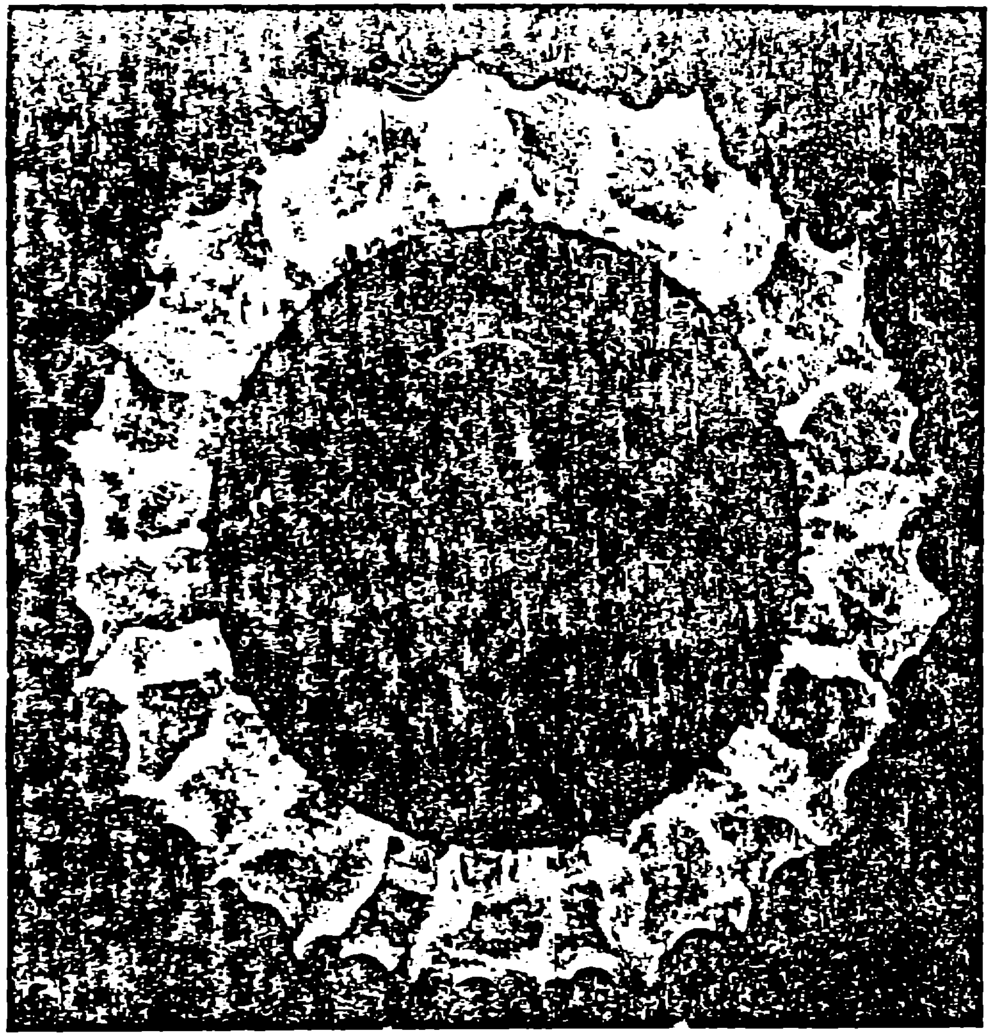

Figure 7A.

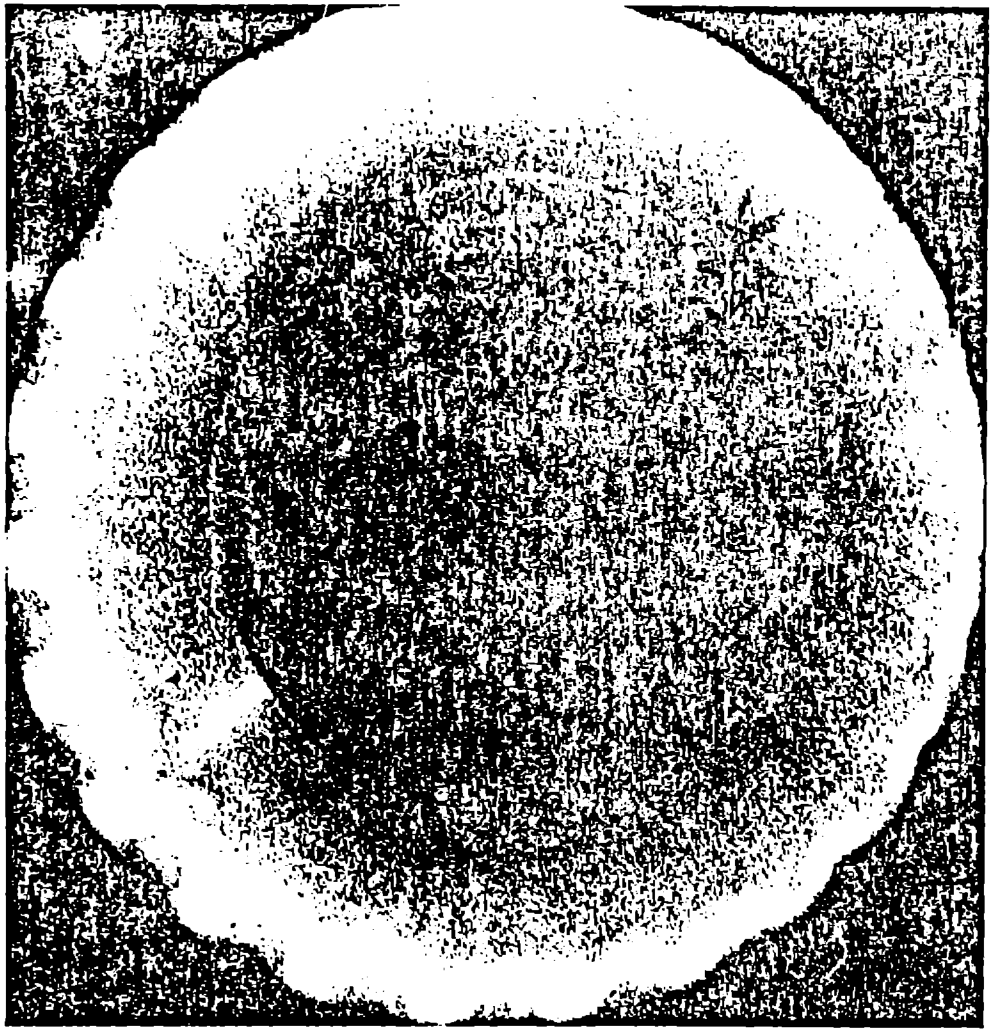

Figure 7B.

Figure 8A.

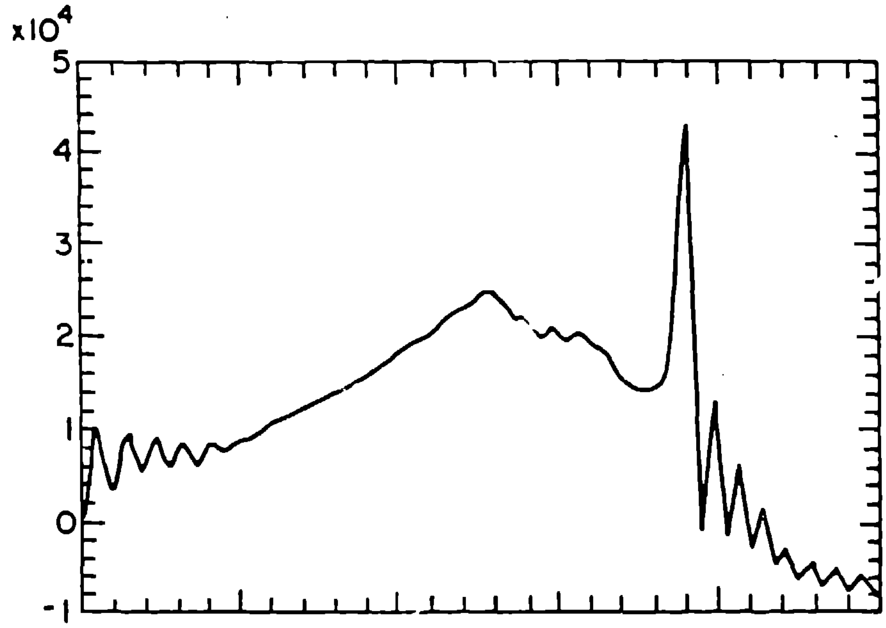

Figure 8B.

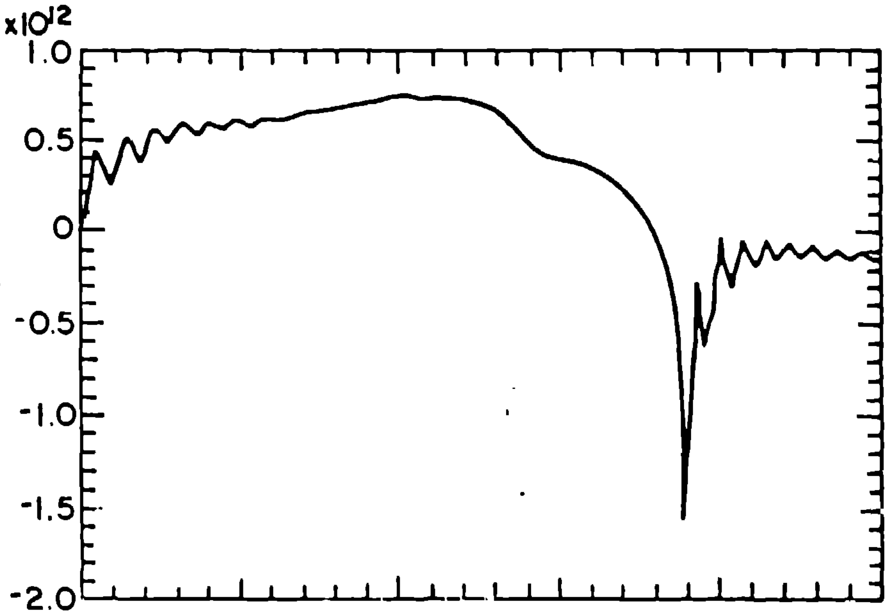

Figure 8C.